



DEVELOPMENT OF PROPORTIONAL COUNTERS USING PHOTSENSITIVE  
GASES AND LIQUIDS\*

D. F. Anderson

October 1984

\*Invited talk presented at the 1984 IEEE Nuclear Science Symposium, Orlando, Florida, October 31-November 2, 1984.



# Development of Proportional Counters Using Photosensitive Gases and Liquids

D. F. Anderson  
Fermi National Accelerator Laboratory  
Batavia, IL. 60510

## Abstract

An introduction to the history and to the principle of operation of wire chambers using photosensitive gases and liquids is presented. Their use as light sensors coupled to Gas Scintillation Proportional Counters and  $\text{BaF}_2$ , as well as their use in Cherenkov Ring Imaging,<sup>2</sup> is discussed in some detail.

## 1. INTRODUCTION

In recent years there has been a great deal of effort spent on the development of photosensitive wire chambers. Although the field has a long history, the renewed interest can be traced back to the work of Seguinot and Ypsilantis. They suggested adding a photosensitive gas to a proportional counter, fitted with a UV transparent window, as a means of detecting the UV photons produced as Cherenkov radiation in gases.

To demonstrate their idea, they constructed the instrument shown in Fig. 1. The light source consisted of a volume of pure argon excited by an alpha source. This produces light in the 9-11 eV range. The detector was a multiwire chamber filled with argon,  $\text{CO}_2$ , and benzene. The photosensitive material was benzene with a threshold for the photoelectric effect of 9.15 eV (1355 Å). With this setup, they were able to show that single photon counting was possible.

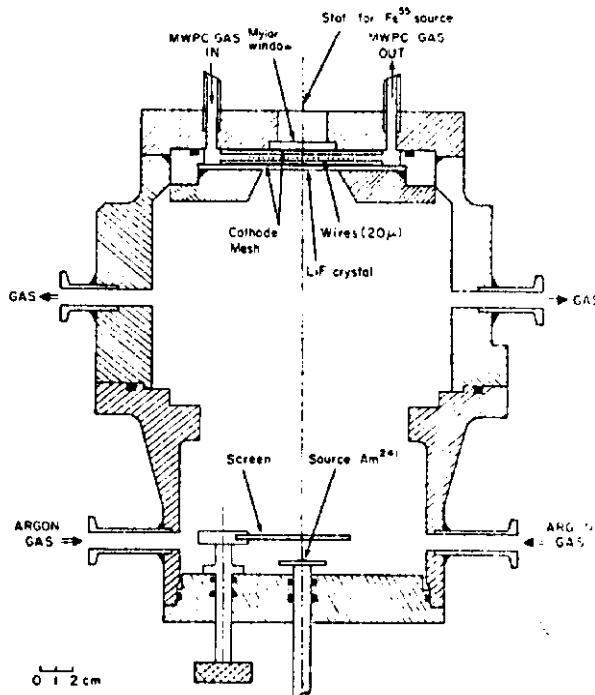


Fig. 1 Photosensitive proportional counter and UV generator

At the same time as the above work, the use of photosensitive proportional counters was suggested independently by Bogomolov, Dubrovskii and Peskov for plasma studies.<sup>2</sup> They demonstrated their idea with a small multiwire chamber with a LiF window, filled with helium and toluene vapors. Toluene has an ionization threshold of 8.5 eV (1460 Å).

The development of wire chambers using photosensitive gases, and later photosensitive liquids, has gone in three major directions. The first, is as a replacement for photomultiplier tubes, PMT, for gas scintillation proportional counters. The second, is for Ring Imaging Cherenkov detectors. The third, is as the photon sensor for the scintillator  $\text{BaF}_2$ . We will discuss all three fields here; although it is not possible to cover these topics completely in a work of this length. In particular, the field of Cherenkov detectors, which has been reviewed elsewhere,<sup>3,4</sup> will be the least complete. A fairly complete bibliography will be provided. We will also restrict ourselves to detectors that detect light, and are not just moderated by photons such as multistep avalanche detectors.<sup>5</sup>

## 2. GSPC

A gas scintillation proportional counter, GSPC, is a type of proportional counter with an energy resolution for X rays a factor of two better than conventional wire chambers. Although the designs of the GSPC vary dramatically, the principle is best exhibited in the parallel plate design in Fig. 2.

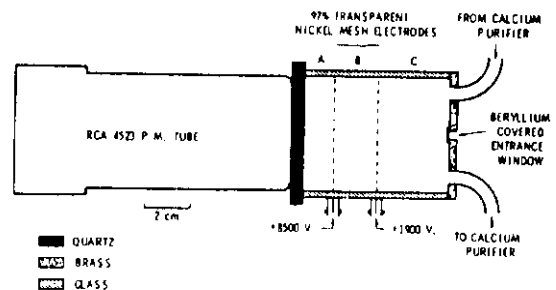


Fig. 2 Parallel plate gas scintillation proportional counter

The GSPC consists of a volume of pure noble gas, usually at 1 atm. Region C of Fig. 2 is an absorption region, deep enough to stop entering X rays. The primary electrons liberated by the X ray are drifted out of this region by a small electric field and into region B. Here the electric field is adjusted such that the electrons gain enough energy between collisions with the gas, to excite the atoms but not ionize them. The excited atoms form a Rydberg molecule which de-excites giving a broad continuous spectrum. The emission spectra of argon, krypton and xenon are shown in Fig. 3. The UV light is then either converted in a wavelength shifter and detected by a glass PMT or detected directly by a quartz PMT. (See Refs. 8 and 9 for a review on this GSPC.)

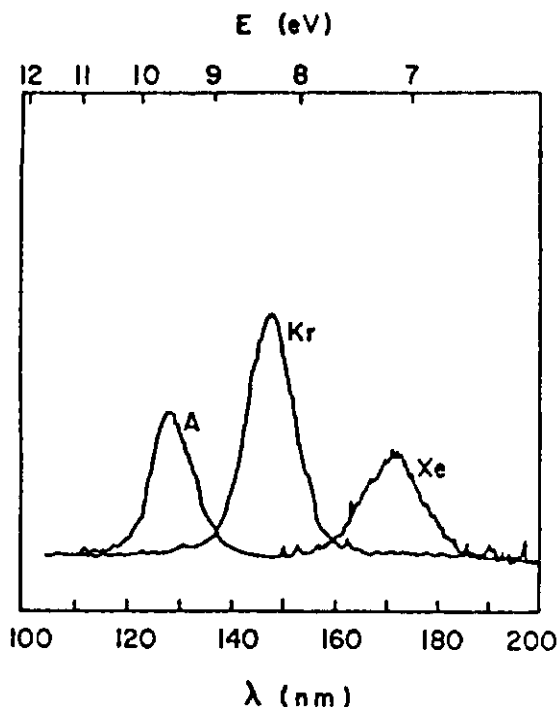


Fig. 3 Argon, krypton and xenon emission spectra<sup>7</sup>

The noble gas of choice for GSPC's has been xenon. This is because of its high X-ray stopping power and its higher UV photon yield. Also, its softer spectrum makes light detection easier. But, the quartz PMT's used are very expensive and greatly limit detector design.

It was first suggested by Policarpo<sup>10</sup> that a photosensitive wire chamber or photo-ionization detector, PID, could be used to replace the PMT for a GSPC. This would offer an instrument with the energy resolution of a GSPC, and the imaging capabilities of a wire chamber. Such an instrument should also be less expensive to construct and be much less sensitive to magnetic fields.

The first coupling of a GSPC to a photosensitive detector was achieved by Peskov.<sup>11,12</sup> The instrument, shown in Fig. 4, was a hybrid using two PMTs at the side of the GSPC, filled with argon plus a little xenon, for the energy determination. The position of an event was determined by an array of "end" type proportional counters looking from below. The photosensitive gas used was trimethylamine, sensitive in the 1050-1550 Å region.<sup>11</sup> An energy resolution of 12% FWHM was measured for 5.9 keV X rays, with a position resolution of about 0.3 mm. The energy resolution was improved to 9.7% FWHM with the use of a Penning gas mixture, differentially mixed.

The first demonstration of a true PID coupled to a GSPC was made by Charpak, Policarpo, and Sauli.<sup>9</sup> Their instrument is shown schematically in Fig. 5. The PID used triethylamine, TEA, with a threshold of 7.5 eV (1653 Å) as the photosensitive gas. The gas mixture was 83% argon, 3% TEA, and 14% methane. Because of the high threshold of TEA, the GSPC gas was Kr and a LiF window separated the two sections. They measured an energy resolution of 10.8% FWHM for 5.9 keV X rays. This same group had first introduced TEA for Cherenkov Ring Imaging with Ypailantis.<sup>13</sup>

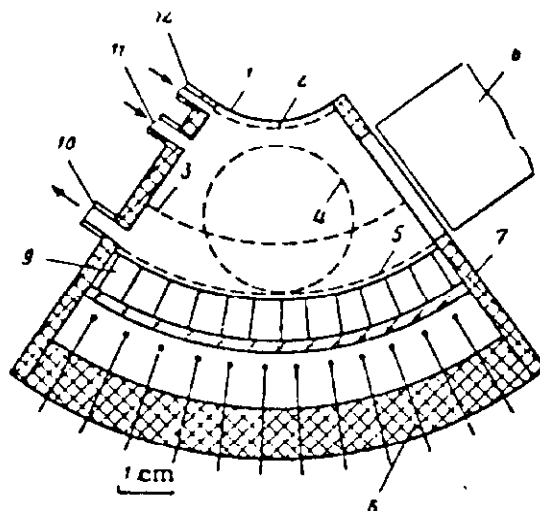


Fig. 4 Gas scintillation proportional counter with PMT readout and photosensitive "end"-type proportional counter<sup>11</sup>

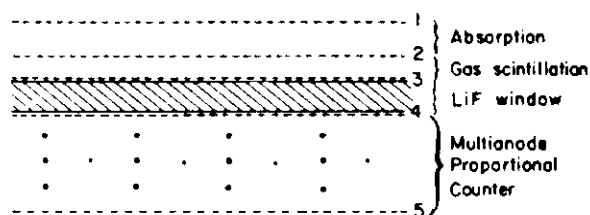


Fig. 5 Gas scintillation proportional counter, coupled to a photo-ionization detector<sup>7</sup>

The use of xenon as the GSPC gas was made possible by the introduction, by Anderson,<sup>14</sup> of tetrakis(dimethylamino)ethylene, TMAE, with a threshold of only 5.36 eV (2315 Å). This lower threshold has the additional advantage of allowing quartz windows to be used which are considerably more rugged and less expensive than the fluoride windows used with the other photosensitive gases.

The detector used in the above work is shown in Fig. 6. The PIPS was filled with 90% argon and 10% methane (P-10). Because of the low vapor pressure of TMAE (0.38 Torr at 21°C<sup>15</sup>) it made up only 0.05% of the gas. The GSPC was a curved grid type with a 1 atm filling of pure xenon. An energy resolution of 9.5% FWHM was measured for 5.9 keV X rays.

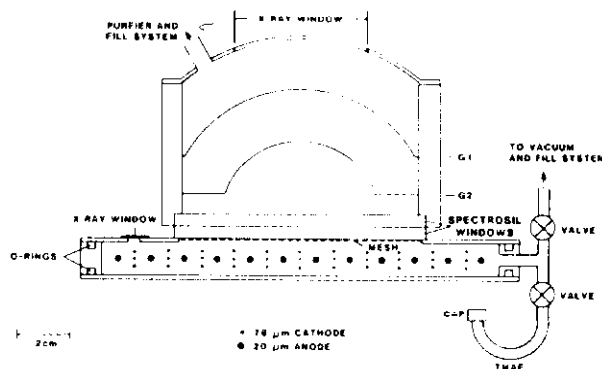


Fig. 6 Curved grid gas scintillation proportional counter coupled to a photo-ionization detector<sup>14</sup>

The absorption length in TMAE of xenon light filtered by a quartz window was also measured. Although the average cross section was estimated at 38 Mb, its low vapor pressure yield an absorption lengths of 23 mm and 11 mm at 20°C and 30°C, respectively. This is much longer than the submillimeter absorption length typical for TEA.

The next logical step in the development of PID's coupled to GSPC was made by Ku and Hailey.<sup>17</sup> They built the first imaging PID. Their detector is shown in Fig. 7. The PID was a multiwire proportional counter with the event position determined from the induced signal on orthogonal cathode planes. The PID gas mixture was 0.3 Torr of TMAE and 580 Torr of P-20. The GSPC was filled with 1 atm of xenon.  $\text{CaF}_2$  was used for the window between the two detectors. An energy resolution of 9% FWHM was measured for 5.9 keV X rays, and a position resolution of 0.9 mm was achieved. They also tested the same instrument with krypton in the GSPC and TEA as the photosensor. Although the induced signal in the PID was narrower due to its shorter absorption depth, the position resolution measured was not better than with TMAE.

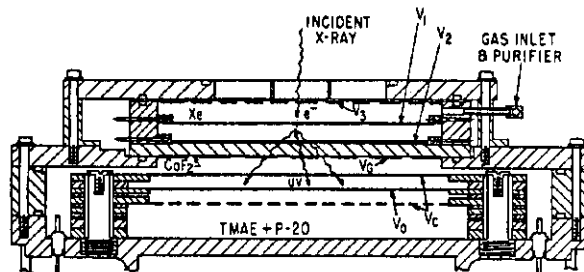


Fig. 7 Imaging gas scintillation proportional counter

As an example of the kind of energy resolution possible with a GSPC coupled to a PID, Fig. 8 shows an X-ray pulse height spectrum from unpublished work by Anderson. The GSPC was filled with xenon and an imaging PID with TMAE was used. The X-ray source is  $^{55}\text{Fe}$  at 5.9 keV, yielding an energy resolution of 7.9% FWHM. Note that the K<sub>α</sub> line at 6.4 keV is starting to be resolved at the right. This is as good as the best measurements made with a PMT.

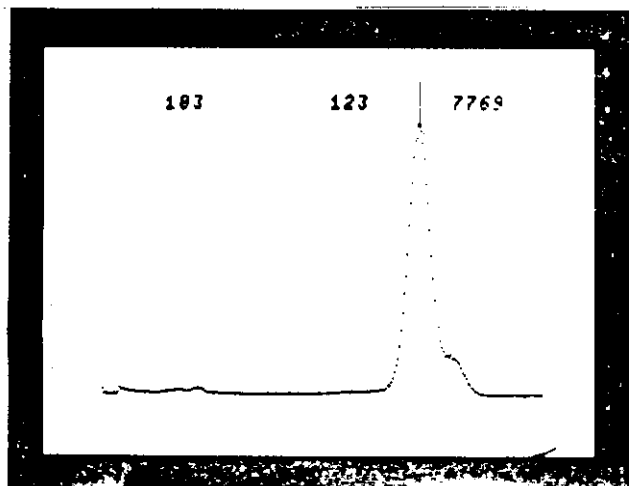


Fig. 8  $^{55}\text{Fe}$  pulse height spectrum

### 3. CHERENKOV RING IMAGING

The second major application of photosensitive wire chambers is particle identification using Ring Imaging Cherenkov RICH detectors. When a charged particle with velocity  $\beta$  ( $\beta = v/c$ ) passes through an optical medium, with index of refraction  $n$ , it emits UV photons at an angle  $\theta_c$ , given by the Cherenkov relation:

$$\cos \theta_c = 1/\beta n,$$

for  $\beta n > 1$ . The photons emitted along the particle path are reflected by a spherical mirror of radius  $r$  onto a focal surface of radius  $r/2$ . (See Fig. 9.)

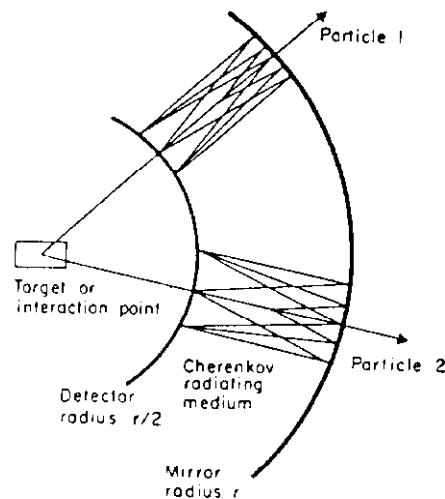


Fig. 9 Schematic of ring-imaging Cherenkov experiment

These photons fall on a circle of radius

$$R = \frac{r}{2} \tan \theta_c.$$

As was first suggested by Seguinot and Ypsilantis,<sup>1</sup> a photosensitive proportional counter placed at the surface of radius  $r/2$  could measure the value of  $R$ . Thus one knows the  $\beta$  of the particle. With a separate measurement of the particle momentum, the particle can be identified. It should also be noted that since the trajectory of the particle, and therefore the center of the Cherenkov ring, can often be determined by external measurements, a single detected photon is often enough to identify a particle.

An important parameter for RICH detectors is the number of photons detected. This number can be calculated from

$$N = N_0 L \sin^2 \theta_c,$$

where  $L$  is the length of the radiator. The figure of merit,  $N_0$ , gives the spectral response of the detector to the Cherenkov radiation. (Also see Ref. 18.)

As with the work done simultaneously with the GSPC, the introduction of the new photosensitive gases defined the UV transparent windows used as well as the radiators. For reference Fig. 10 shows the absorption spectra of four photosensitive gases<sup>19</sup> and the transmission of the UV windows available.

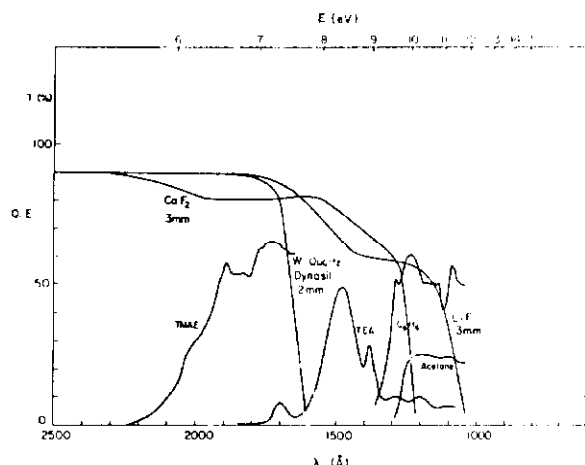


Fig. 10 Absorption spectra of some photosensitive gases and transmissions of UV windows

### 3.1 Spark Chamber Readout

The first work in RICH detectors was done with simple wire chambers with one-dimensional readouts.<sup>20,21</sup> The first two-dimensional Cherenkov ring was recorded by Charpak et al.,<sup>3</sup> with a wire chamber employing a spark chamber and video readout. Figure 11 shows a schematic of their detector. The instrument was a multistep avalanche chamber with a triggered spark chamber as a second step, separated by a drift region to prevent photon feedback and to allow for triggering time. The gas filling was helium with about 5% TEA. A  $\text{CaF}_2$  window was used. Entering UV photons were converted to electrons by the TEA. These electrons were amplified in the first step of the detector which then caused a spark which was read out at the back by a TV camera.

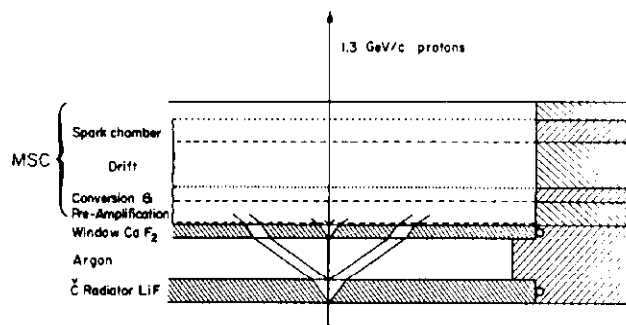


Fig. 11 Schematic of ring-imaging Cherenkov detector experiment

Two Cherenkov radiators were used in the first test: a 5 mm thick LiF radiator, and then a 1 m long argon radiator in the configuration of Fig. 12. For 1.5 GeV/c protons they detected 1.7 photons per event with the argon radiator. The integrated image of 30 events is shown in Fig. 13. The spot in the center is due to the direct ionization of the beam particles. The ring radius was  $R = 24.42 \pm 0.22$  mm with a standard deviation of 2.05 mm.

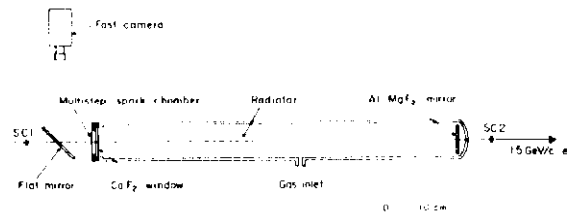


Fig. 12 Experimental Cherenkov setup with argon radiator

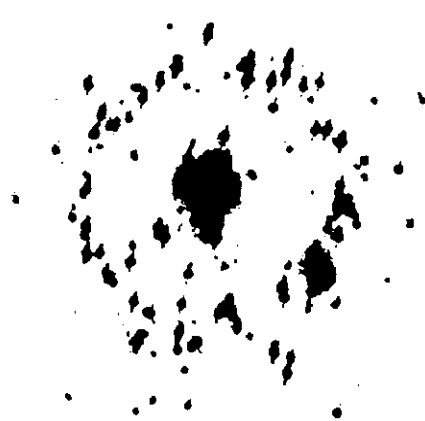


Fig. 13 Cherenkov ring for 30 events with 1.5 GeV/c protons

In later work the same group measured an average of 6.8 photons per event, for 10 GeV/c pions, with the radiator filled with 1.6 atm of argon. This yields an  $N_0$  of 80  $\text{cm}^{-1}$ . In this work they also made the first demonstration of TMAE in a RICH detector.

### 3.2 Cathode Readout

The first RICH detector used in an actual high energy physics experiment is in experiment E-605 at Fermilab.<sup>22,23</sup> Two detectors are used with a single 15 m long helium radiator at 1 atm, used to identify hadrons between 50 and 200 GeV/c. The detectors consist of two multistep proportional counters each with an active area of 40 x 80  $\text{cm}^2$ .

The photosensitive gas used is TEA (3%) with helium (97%). The UV windows are made of  $\text{CaF}_2$ , consisting of a mosaic of 10 x 10  $\text{cm}^2$  crystals. The detectors have absorption, preamplification and transfer regions, followed by a multiwire proportional counter. Cathode readouts give the x- and y-coordinate of the event, while the direct anode pulse provides the u-coordinate.

For 70 GeV/c pions they measured an average of 2.5 detected photons per ring, or  $N_0 = 24 \text{ cm}^{-1}$ . The measured position resolution was 2 mm FWHM with an average ring radius of 67 mm. The predicted Cherenkov ring centers of all identified particles hitting one of their mirrors are superimposed in Fig. 14.<sup>23</sup> There are about 1000 events with kaons visible inside a pion ring.

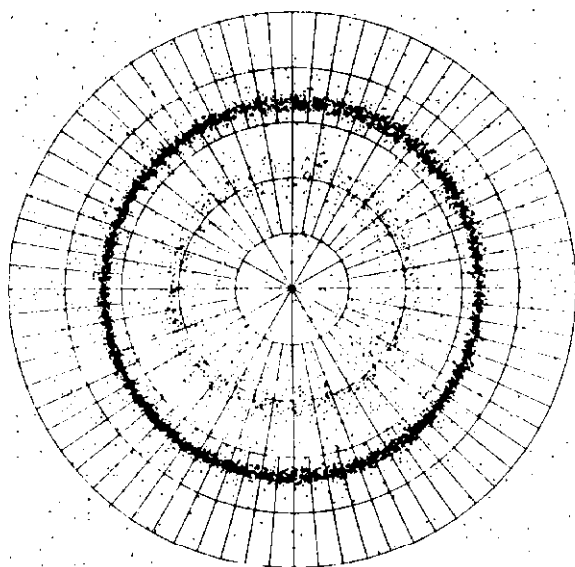


Fig. 14 Cherenkov events from E-605<sup>23</sup>

Another technique has been used by Contrakon, et al.<sup>24</sup> They built a test proportional counter with a combination of anode wire and cathode pad readout, using a  $18 \times 18 \text{ cm}^2$   $\text{CaF}_2$  window. The gas filling was  $\text{CH}_4$  (97%) and TEA (3%).<sup>2</sup> For their test they used a Cherenkov radiator consisting of 5 m of argon (20%) and helium (80%) at 1 atm. For 100 GeV/c muons they detected an average of about 4 photons per event, or  $N_0 = 40 \text{ cm}^{-1}$ . Their position resolution was 4 mm FWHM with a ring size of  $R = 70 \text{ mm}$ .

### 3.3 TPC

Another technique used for RICH detectors is the Time Projection Chamber, TPC, shown schematically in Fig. 15.<sup>25</sup> The electrons forming the Cherenkov ring are drifted sideways into a multiwire proportional counter. The y-coordinate of an electron is determined by the wire struck. The x-coordinate is given by the arrival time of the electron. The advantage of such a scheme is that a much larger number of electrons can be detected per ring with a small number of channels. The disadvantage is that with a typical drift velocity of 5-10 cm/ $\mu\text{s}$  for the electrons, a large detector will require a fairly long time between particles. This technique was first suggested for RICH applications and tested with a one-dimensional detector by Ekelof, et al.<sup>26</sup>

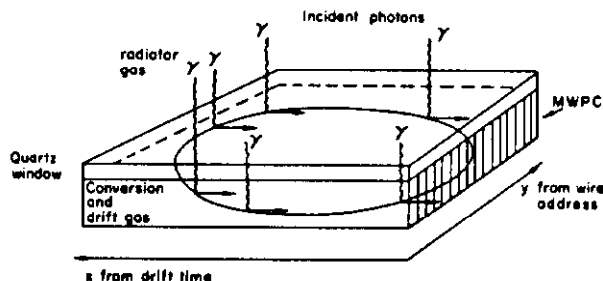


Fig. 15 Schematic of a time projection chamber for Cherenkov ring imaging<sup>15</sup>

Cherenkov detectors using TPC readouts have been designed for a Delphi detector at LEP (CERN) and for the Omega spectrometer at CERN. A test of the Omega RICH detector has been carried out.<sup>27</sup> The photon detectors use TMAE with two quartz windows  $80 \times 20 \text{ cm}^2$ . The electrons are drifted towards the center with a maximum drift of 20 cm. With a 2 m long argon radiator, they measured an average of 3.2 photons per 10 GeV/c pions with a position resolution of 1.7 mm FWHM. Their final design with a 5 m Cherenkov radiator is now in operation. (See P.H. Sharp, these proceedings.)

A test detector<sup>28</sup> for the Delphi experiment has also been tested.<sup>28</sup> It consisted of a TPC with a  $20 \times 20 \text{ cm}^2$  quartz window. The gas mixture was methane (80%), isobutane (20%), and TMAE. The Cherenkov radiator was 50 cm of isobutane. With 10 GeV/c negative particles, they detected an average of 10 photons per event yielding an  $N_0 = 72 \text{ cm}^{-1}$ . The final design with a 170 cm drift is presently under test. (See T. Ypsilantis, these proceedings.)

### 3.4 Needles

The work on needle detectors for Cherenkov experiments has been directed by G. Comby<sup>29</sup> at Saclay, although their use was first suggested for RICH by Seguinot and Ypsilantis. The photoelectrons are amplified in the strong field at the end of a needle (see Fig. 16), giving a large signal. The advantage is that a large number of photons can be detected at once. The disadvantages are that they are difficult to construct, the spacial resolution is limited to the cell size, and a great deal of electronics is necessary.

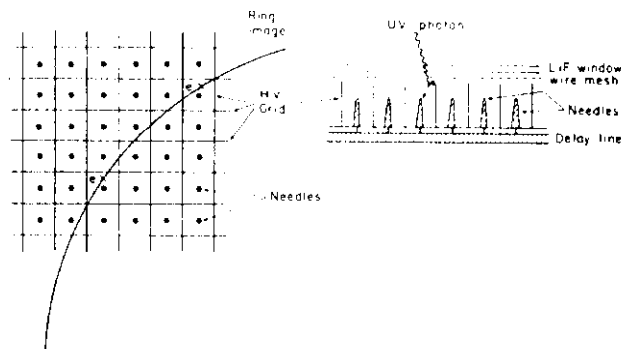


Fig. 16 Schematic of a needle detector for Cherenkov ring imaging

There were constructed instruments with up to 2500 needles with different needle spacings. With an instrument of 1008 needles, a  $\text{CaF}_2$  window, and using TEA as the photosensitive material, the light produced by 6 GeV/c pions in a 93 cm argon radiator was detected. They measured an average of 0.4 photoelectrons per event, or  $N_0 = 28 \text{ cm}^{-1}$ .

### 3.5 Low Pressure RICH

One problem that has faced RICH detectors is that a high energy particle passing through the detector liberates on the order of  $10^3$  electrons. In a detector designed to detect one electron, this can be a serious problem, and often causes sparking or photon feedback. To avoid this, most detectors have either been operated out of the beam or with the region of the beam inactive in the detector. But, even these solutions are ineffective for the particles in the beam halo.

To address this problem the Charpak group at CERN<sup>30</sup> has constructed a small test low pressure chamber with an absorption, a preamplification and a transfer region. This was followed by a multiwire proportional counter in one configuration. In a second design, they used a parallel plate region and a 2 x 2 cm<sup>2</sup> "wedge and strip" printed circuit readout.<sup>31</sup> The detector had a CaF<sub>2</sub> window. The gas fillings were TMAE plus 5 to 20 Torr of pure isobutane. For single photons they measured a high detection efficiency and better than 1 mm FWHM position resolution.

The advantage of operating a RICH detector at such a low pressure is that it reduces the amount of charge liberated by a passing particle by up to two orders of magnitude. Also the use of "wedge and strip" cathode readouts allow high event multiplicity with much fewer channels for a non-TPC design.

Also see Ref. 32 for additional works on the subject of RICH.

#### 4. BaF<sub>2</sub> SCINTILLATOR

With the introduction of TMAE, with its low photo-ionization threshold, it was natural to search for a solid scintillator that emitted light in a region detectable by the gas. The first, though marginal, success was reported by Anderson.<sup>15</sup> The scintillator was BaF<sub>2</sub>, which to date, emits light of the shortest wavelength found. It is also the only solid scintillator yet to be coupled to a photosensitive gas, though the search goes on.

As a scintillator, BaF<sub>2</sub> has many desirable characteristics. As a comparison, Table I lists some properties of BaF<sub>2</sub> along with those of BGO and NaI(Tl).<sup>33</sup> Unlike the other two, BaF<sub>2</sub> has two emission maxima. The shorter component peaks at 225 nm and contains about 20% of the light. This component also has a decay constant 1000 times faster than those of long component and about 500 times faster than those of BGO and NaI(Tl). Thus the short component is often referred to as the fast component.

Table I

Properties of Three Scintillators

	BaF <sub>2</sub>	BGO	NaI(Tl)
Density (g/cm <sup>3</sup> )	4.9	7.1	3.7
Radiation length (cm)	2.1	1.1	2.6
dE/dx (min)(MeV/cm)	~6	8	4.8
Linear attenuation coefficient at 511 keV (cm <sup>-1</sup> )	0.47	0.92	0.34
Peak emission (nm)	225 310	480	410
Decay constant (ns)	0.6 620	300	250
Index of refraction	1.56	2.15	1.85
Light yield (photons/MeV)	2x10 <sup>3</sup> 6.5x10 <sup>3</sup>	2.8x10 <sup>3</sup>	4x10 <sup>4</sup>
Hygroscopic	No	No	Yes

Ref. 33.

In the first work, a small BaF<sub>2</sub> crystal was coupled to a single wire proportional counter filled with TMAE, argon (90%) and methane (10%) at 600 Torr. For gamma rays in the 1 MeV range, detection

efficiencies were measured at a few percent. This poor efficiency was due to the small overlap of the BaF<sub>2</sub> spectrum with the detection response of TMAE in the gas phase, and to the poor light collection efficiency of the first setup.

#### 4.1 Liquid Photocathode

In an attempt to improve the photon detection efficiency for BaF<sub>2</sub>, a "liquid" photocathode was conceived.<sup>34</sup> It is quite easy to calculate the ionization threshold,  $E_{TH}$ , for liquid TMAE (electrons detected in the liquid) and for a liquid TMAE photocathode,  $E_{LPC}$ .<sup>35,36</sup> These are given by

$$E_{TH} = IP + P_+ + V_0$$

and

$$E_{LPC} = IP + P_+ \quad (\text{for } V_0 < 0).$$

Here IP is the ionization potential in the gas phase and  $P_+$  is the polarization energy of the positive ion.  $V_0$  is the ground-state energy, with respect to the vacuum, of a free electron in the liquid. Using the value  $V_0 = -0.28$  eV<sup>37</sup> and the estimate of  $P_+ = -1.26$  eV, we have  $E_{TH} = 3.82$  eV (3246 Å) and  $E_{LPC} = 4.0$  eV (3100 Å). The reason the photocathode threshold is higher is because the electrons released in the liquid must overcome  $V_0$  to escape. Thus there are low energy electrons in the liquid that, in principle, could be drawn from the surface if the electric field were high enough.

The first liquid photocathode is shown in Fig. 17. It consisted of a water-cooled copper plate for condensing the TMAE and a low-pressure wire chamber. The TMAE is extremely thin on the surface and thus the instrument can be operated in any orientation. The optical window was made of quartz. The counter gas was only 3 Torr of isobutane to increase the photoelectron collection efficiency. In that work, the counter was operated warm with the photocathode kept at 18°C. Using filters, a threshold of about 4.3 eV was estimated, and a much higher efficiency for the light from BaF<sub>2</sub> was also measured. The estimated quantum efficiency for the short component of BaF<sub>2</sub> was about 4%.

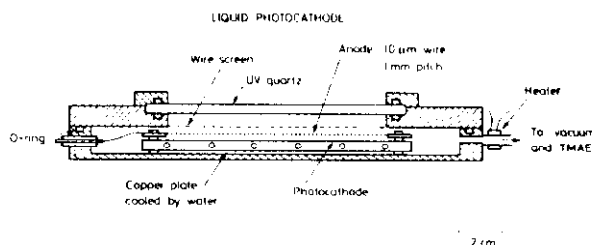
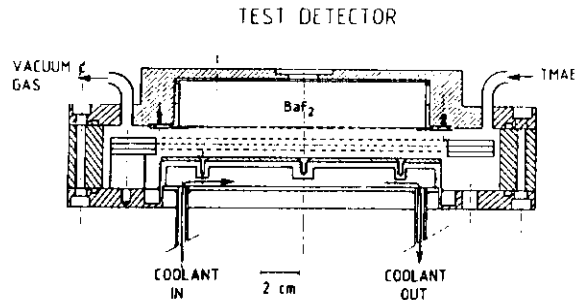


Fig. 17 Liquid photocathode<sup>34</sup>

A second instrument was made that incorporated a BaF<sub>2</sub> crystal, 2.5 cm thick and 12 cm in diameter, as shown in Fig. 18.<sup>38</sup> Again a low pressure counter was used, filled with 3 to 9 Torr of isobutane. This low pressure makes the wire chamber insensitive to the passing particles, while enhancing the sensitivity to UV photons. The TMAE was condensed on a cold surface at 2°C.

Using 350 MeV alpha particles, the electron component of the signal had a rise time of only 10 ns, and the ion drift time was only slightly over 1 µs. A timing resolution of 540 ps FWHM was achieved. An energy resolution of 28.5% FWHM was also measured for



DETAIL OF TEST DETECTOR

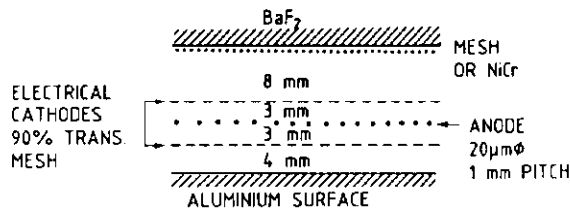


Fig. 18  $\text{BaF}_2$  coupled to a liquid photocathode<sup>38</sup>

970 MeV protons losing about 18 MeV in the crystal. Using the same instrument with a cathode pad readout, a position resolution of about 3 mm FWHM was measured.

The estimated number of photons detected in this final configuration was approximately  $10^4$  per GeV. It is expected that if the electric field at the surface of the liquid photocathode is increased, this number in principle could be increased.

#### 4.2 Adsorption and Gas

It was noted<sup>38</sup> that when TMAE is added to a detector, all the metallic surfaces become photosensitive. To utilize this effect, a complete  $\text{BaF}_2$  calorimeter tower was constructed,<sup>39</sup> that used TMAE and low pressure chambers, but without cooling. A schematic of the tower is shown in Fig. 19. The instrument consisted of 14 crystals varying in thickness from 1 cm to 5 cm. All were 12.6 cm in diameter. The total thickness of  $\text{BaF}_2$  was 40.5 cm, making 19.3 radiation lengths. Each crystal was preceded by its own wire chamber. The surfaces of the  $\text{BaF}_2$  crystals were coated with a 15 Å layer of NiCr, which is a UV transparent conductive coating. When TMAE is introduced into the detector, the adsorbed gas acts as a photocathode. There is also some contribution from the gas volume. But the amplification in a low pressure chamber is almost parallel plate amplification. Thus the contribution from gas is probably fairly small.

The pulse-height spectra for 108 MeV and 200 MeV electrons are shown in Fig. 20. The resolutions are 30% and 20% FWHM, respectively. But when correcting for the energy leakage out the side of the tower, a resolution of  $\sigma/E = 2.5\% E^{1/2}$  (GeV) was determined. This correction was made using the EGS Monte Carlo simulation program.

The energy deposit per crystal is shown in Fig. 21 for 108 MeV and 200 MeV electrons, as well as for 108 MeV/c pions and muons. The energy deposited in crystal 6 appears low because it is 1 cm thick and the surrounding crystals are 2.5 cm thick. This

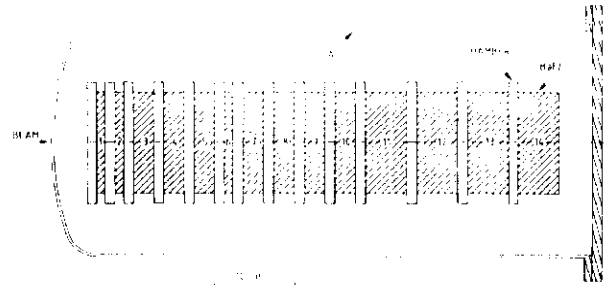


Fig. 19  $\text{BaF}_2$  coupled to a liquid photocathode<sup>38</sup>

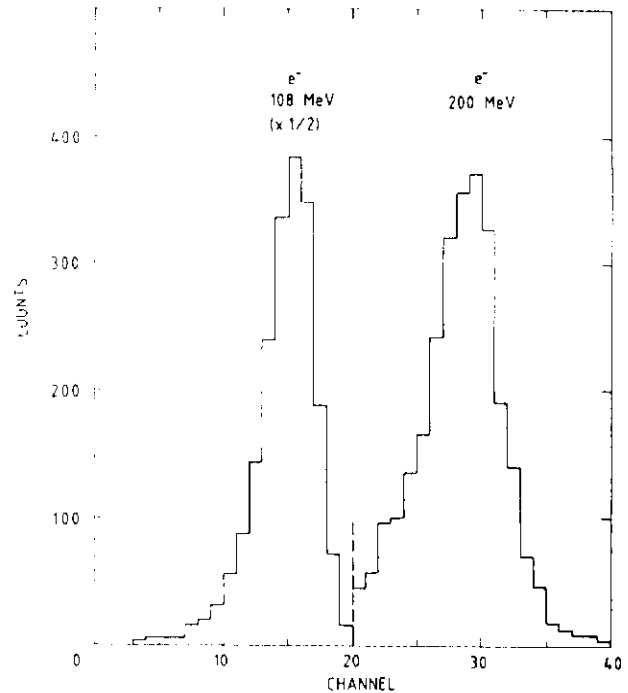


Fig. 20 Pulse height spectra for 108 MeV and 200 MeV electrons<sup>39</sup>

figure shows the advantage of using wire chambers over phototubes. One can achieve high segmentation and measure both the lateral and longitudinal development of the shower.

In a new work by the Charpak group,<sup>40</sup> the effect of increasing the temperature of the detector to increase the TMAE pressure was measured. They found that the energy resolution for 662 keV gamma rays increases up to around 70°C and then remained constant. The limiting resolution was 81% FWHM.

For a review on the subject of low pressure counters, see Refs. 41 and 42.

#### 5. CONCLUSION

The modern field of proportional counters using photosensitive gases and liquids is a new one, with a growing number of applications and investigators. Chambers of a large fraction of 1 m<sup>2</sup> are now possible with quantum efficiencies approaching 50%, and with millimeter position resolution. Only the three major applications of the GSPC, RICH and  $\text{BaF}_2$  have been addressed here. The techniques being developed are certainly applicable to other fields such as the counting of Lyman Alpha photons in atomic physics.



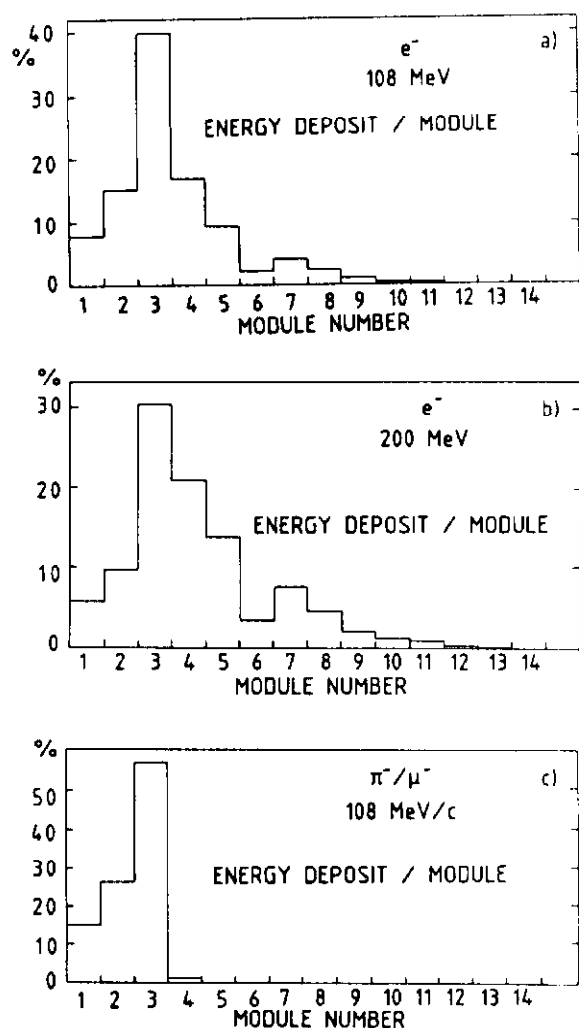


Fig. 21 Energy deposit per crystal for 108 MeV electrons, 200 MeV electrons, and 108 MeV/c pions and muons. Crystal 6 is only 40% as thick as its neighbors.

The study of photosensitive gases and liquids is in need of much good academic work. Much of the existing work has been done by pragmatic investigators with a specific problem to solve. And thus, they were often denied the luxury of careful academic studies. (The work of T. Ypsilantis and collaborators is a marked exception.) Academic institutions should be encouraged to become involved. An example of a subject that would be suitable for academic study is the liquid photocathode. Such questions as spectral response, the effect of temperature, and the role of the electric field are yet untouched.

#### REFERENCES

1. J. Seguinot and T. Ypsilantis, Nucl. Instrum. Methods **142** (1977) 377.
2. G. D. Bogomolov, Yu. V. Dubrovskii and V. D. Peskov, Instrum. Exp. Tech. **21** (1978) 778.
3. G. B. Coutrakon, IEEE Trans. Nucl. Sci. **NS-31** (1984) 27.
4. T. Ypsilantis, "Ring Imaging Cerenkov Counters," IEEE Trans. Nucl. Sci. **NS-32** (1985).

5. G. Melchart, G. Charpak and F. Sauli, IEEE Trans. Nucl. Sci. **NS-27** (1980) 124.
6. H. E. Palmer, IEEE Trans. Nucl. Sci. **NS-22** (1975) 100.
7. G. Charpak, A. Palicarpo and F. Sauli, IEEE Trans. Nucl. Sci. **NS-27** (1980) 212; M. Alegria Feio et al., Nucl. Instrum. Methods **176** (1980) 473; M. Saleta S.C.P. Leite et al., Nucl. Instrum. Methods **179** (1981) 295.
8. A. J. P. L. Policarpo, Space Sci. Instrum. **3** (1977) 77.
9. D. F. Anderson, "Gas Scintillation Proportional Counters," Proceedings of the 1981 INS International Symposium on Nuclear Radiation Detectors, Tokyo, 23-26 March, 1981.
10. A. J. P. L. Policarpo, Nucl. Instrum. Methods, **153** (1978) 389.
11. V. D. Peskov, Instrum. Exp. Tech. **23** (1980) 507.
12. G. F. Karabadzha, V. D. Peskov and E. R. Podolyak, Nucl. Instrum. Methods, **217** (1983) 56.
13. G. Charpak et al., Nucl. Instrum. Methods **164** (1979) 419; G. Charpak et al., Nucl. Instrum. Methods **180** (1981) 387.
14. D. F. Anderson, Nucl. Instrum. Methods **178** (1980) 125.
15. D. F. Anderson, IEEE Trans. Nucl. Sci. **NS-28** (1981) 842.
16. D. F. Anderson et al., Nucl. Instrum. Methods **163** (1979) 125.
17. William H.-M. Ku and Charles J. Hailey, IEEE Trans. Nucl. Sci. **NS-28** (1981) 830; C. J. Hailey, W. H.-M. Ku and M. H. Vartanian, "An Imaging Gas Scintillation Proportional Counter for the Detection of Subkilo-electron-volt X-rays", paper presented at "Workshop on X-ray Astronomy and Spectroscopy." Held at the NASA Goddard Space Flight Center, Greenbelt, MD, 5-7 October 1981. Columbia Astrophysics Lab Contribution No. 214; William H.-M. Ku, Charles J. Hailey and Michael H. Vartanian, Nucl. Instrum. Methods **196** (1982) 63.
18. J. Seguinot, J. Tocqueville and T. Ypsilantis, Nucl. Instrum. Methods **173** (1980) 283.
19. A. Breskin et al., IEEE Trans. Nucl. Sci. **NS-28** (1981) 429.
20. R. S. Gilmore et al., Nucl. Instrum. Methods **157** (1978) 507.
21. J. Chapman, D. Meyer and R. Thun, Nucl. Instrum. Methods **158** (1979) 187.
22. M. Adams et al., Nucl. Instrum. Methods **217** (1983) 237; Ph. Mangeot et al., Nucl. Instrum. Methods **216** (1983) 79; G. Coutrakon et al., IEEE Trans. Nucl. Sci. **NS-29** (1982) 323; R. Bouclier et al., Nucl. Instrum. Methods **205** (1983) 403.
23. H. Glass et al., IEEE Trans. Nucl. Sci. **NS-30** (1983) 30.
24. G. Coutrakon, S. Dhawan and M. Izycki, "Cherenkov Ring Imaging Using a Proportional Wire Chamber with Cathode Readout," submitted to Nucl. Instrum. Methods, 1984.
25. E. Barrelet et al., Nucl. Instrum. Methods **200** (1982) 219.
26. T. Ekelof et al., "The Cherenkov Ring-Imaging Detector: Recent Progress and Future Development," CERN-EP/80-115 (1980).
27. M. Davenport et al., IEEE Trans. Nucl. Sci. **NS-30** (1983) 35.
28. L. O. Eek et al., IEEE Trans. Nucl. Sci. **NS-31**, No. 2 (1984) 949.
29. G. Comby and P. Mangeot, IEEE Trans. Nucl. Sci. **NS-27** (1980) 106; G. Comby and P. Mangeot, IEEE Trans. Nucl. Sci. **NS-27** (1980) 111; G. Comby et al., IEEE Trans. Nucl. Sci. **NS-29** (1982) 328.
30. W. Dominik et al., "Possible Applications of Low-Pressure Multistep Chambers to Cherenkov Ring Imaging," presented at the Int. Conf. on

- Instrumentation for Colliding-Beam Physics, Novosibirsk, USSR, 15-21 March 1984, CERN-EP/84-29.
31. C. Martin et al., Rev. Sci. Instrum. 52 (1981) 1067; R. S. Gilmore et al., IEEE Trans. on Nucl. Sci. NS-28 (1981) 435; O. H. W. Siegmund et al., IEEE Trans. Nucl. Sci. NS-30 (1983) 503.
  32. S. Durkin, A. Honma and D.W.G.S. Leith, "Preliminary Results on Tests of a Cherenkov Ring Imaging Device Employing a Photoionizing PWC," SLAC-Pub-2186 (1978); S. H. Williams et al., "An Evaluation of Detectors for a Cherenkov Ring-Imaging Chamber," SLAC-Pub-2412 (1979); G. Charpak and F. Sauli, "Use of TMAE in a Multistep Proportional Chamber for Cherenkov Ring Imaging and Other Applications," CERN-EP/83-128; Stephen H. Williams, "Cherenkov Ring Imaging Detector Development at SLAC," SLAC-Pub-3360 (1984).
  33. M. Laval et al., Nucl. Instrum. Methods 208 (1983) 169; R. Allemand et al., "New Developments in Fast Timing with BaF<sub>2</sub> Scintillator," Communication LETI/MCTE/82-245<sup>2</sup>, Grenoble, France (1982); BGO-NaI(Tl) Comparison, paper distributed at the International Workshop on Bismuth Germanate, Princeton University, 1982; M. R. Farukhi and C. F. Swinehart, IEEE Trans. Sci. NS-18 (1971) 200.
  34. D. F. Anderson, Phys. Lett. 118B (1983) 230.
  35. Y. Nakato, M. Ozaki and H. Tsubomura, J. Phys. Chem. 76 (1972) 2105; R. A. Holroyd and R. L. Russell, J. Phys. Chem. 79 (1983) 483.
  36. D. Anderson et al., Nucl. Instrum. Methods 225 (1984) 8.
  37. R. A. Holroyd and D. Anderson, "The Physics and Chemistry of Room-Temperature Liquid Ionization Chambers," submitted to Nucl. Instrum. Methods (1984).
  38. D. Anderson et al., Nucl. Instrum. Methods 217 (1983) 217.
  39. D. Anderson et al., "Test Results of a BaF<sub>2</sub> Calorimeter Tower with a Wire Chamber Readout," CERN-EP/84-82; submitted to Nucl. Instrum. Methods.
  40. M. Suffert, R. Bouclier and G. Charpak, "Influence of the Temperature on the Response of the Fast Component of BaF<sub>2</sub> Scintillators Coupled to a Photomultiplier of a Photosensitive Wire Chamber," to be submitted to Nucl. Instrum. Methods.
  41. A. Breskin, Nucl. Instrum. Methods 196 (1982) 11.
  42. A. Breskin, G. Charpak and S. Majewski, Nucl. Instrum. Methods 202 (1984) 349.